

## Evidence for a Complex $\vec{L} \cdot \vec{S}$ Interaction in the Deuteron-Nucleus Optical Potential

R. P. Goddard and W. Haeberli  
 University of Wisconsin, Madison, Wisconsin 53706  
 (Received 12 January 1978)

The addition of an imaginary  $\vec{L} \cdot \vec{S}$  interaction to the deuteron-nucleus optical potential significantly improves the fit to cross-section and analyzing-power measurements for elastic scattering of 10–15-MeV deuterons from medium-weight nuclei. The largest improvement results from a shift of the analyzing powers toward smaller angles, relative to the cross section. The imaginary  $\vec{L} \cdot \vec{S}$  potential has the same sign and about one-half the strength of the real  $\vec{L} \cdot \vec{S}$  potential.

Since 1960, when the first polarized ion sources made accurate analyzing power measurements possible, many investigators have used deuteron optical-model calculations to explain the measured cross sections and analyzing powers for deuteron elastic scattering from complex nuclei. In most cases (at least for  $A > 40$  and  $E_d \geq 9$  MeV), qualitative agreement with measured cross sections and vector analyzing powers ( $iT_{11}$ ) has been obtained<sup>1</sup> using potentials which include complex central and real  $\vec{L} \cdot \vec{S}$  components. However, most of these fits are inferior to similar calculations for nucleon scattering (e.g., compare Lohr and Haeberli<sup>1</sup> and Becchetti and Greenlees<sup>2</sup>). More serious difficulties are encountered when the tensor analyzing powers  $T_{20}$ ,  $T_{21}$ , and  $T_{22}$  are considered: Until now, the statement of Keaton and Armstrong<sup>3</sup> that “no one has been able to fit all five observables . . . at any single energy for any target nucleus” has remained true.<sup>4</sup>

The purpose of this Letter is to show that the introduction of an imaginary  $\vec{L} \cdot \vec{S}$  component in the deuteron-nucleus optical potential significantly improves the fit to cross-section and analyzing-power measurements for elastic scattering of 10–15-MeV deuterons from medium-weight nuclei. The most important effect of this new component is to shift the calculated analyzing powers toward smaller angles, without changing the angular position of the cross-section calculations. The beneficial effect of this shift is illustrated in Fig. 1, which shows partial angular distributions, from 60° to 150°, of the cross section and  $iT_{11}$ , for the elastic scattering of 10- and 15-MeV deuterons from three nuclei. The data are from Stephenson,<sup>5</sup> Goddard and Haeberli,<sup>6</sup> and Hardekopf *et al.*<sup>7</sup> The dotted curves are conventional optical-model calculations, which do not include an imaginary  $\vec{L} \cdot \vec{S}$  potential. In each case, the best conventional fit is a compromise between the cross section and  $iT_{11}$ : The cross-section is too far forward in angle, and the analyzing-

power calculation is too far back, in comparison to the measurements. Changes in the usual parameters can shift the cross section and  $iT_{11}$  together toward smaller or larger angles, but such changes cannot shift one observable relative to the other.

The solid curves in Fig. 1 are calculations which include an imaginary  $\vec{L} \cdot \vec{S}$  potential. This new term shifts  $iT_{11}$  forward, and slight adjustments in the remaining parameters (primarily a decrease in the strength of the real central potential) shift the cross section toward larger angles. For all three nuclei, the addition of the imaginary  $\vec{L} \cdot \vec{S}$  potential results in considerably improved agreement with the measurements for at least one of the two observables shown. Some problems still remain, especially in  $iT_{11}$  for <sup>46</sup>Ti, for which both calculations are consistently more negative than the data. Even in this case, however, the agreement with the  $iT_{11}$  data is improved at backward angles and is certainly no worse overall, and the agreement with the cross section is improved substantially.

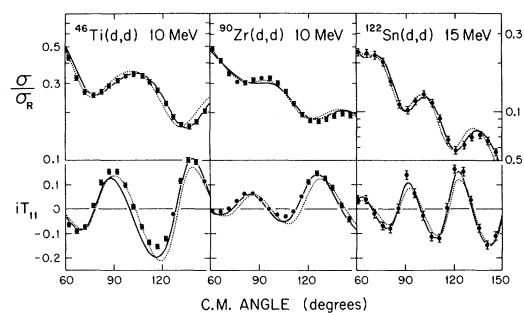


FIG. 1. Details of optical-model calculations for deuteron elastic scattering from <sup>46</sup>Ti at 10 MeV (Refs. 5, 6), <sup>90</sup>Zr at 10 MeV (Ref. 6), and <sup>122</sup>Sn at 15 MeV (Ref. 7), showing the relative angular shift between  $\sigma/\sigma_R$  and  $iT_{11}$ . Here,  $\sigma/\sigma_R$  is the cross section divided by the Rutherford cross section. The curves are optical-model fits including an imaginary  $\vec{L} \cdot \vec{S}$  potential (solid curves) and without it (dotted curves). The potentials are adjusted to optimize the fit to the cross section and all four analyzing powers, including data which are not shown.

In all of the calculations in Fig. 1, the potentials were adjusted by an automatic search routine<sup>8</sup> to optimize the fits to complete angular distributions of the cross sections and all four analyzing powers; the forward- and backward-angle data and the tensor analyzing powers were omitted from the figure to conserve space. Figure 2 shows a complete set of data and calculations, for 15-MeV deuterons on <sup>90</sup>Zr (Ref. 7). The curves have the same meaning as in Fig. 1. The beneficial effects of the imaginary  $\vec{L} \cdot \vec{S}$  potential can be seen in the tensor analyzing powers  $T_{20}$  and  $T_{22}$ , as well as in the cross section and  $iT_{11}$ . The solid curves in Fig. 2 represent the first successful optical-model fit to the cross section and all four analyzing powers for deuteron scattering from any nucleus at energies above the Coulomb barrier.

The parameters describing the potentials used for the solid curves in Fig. 2 are given in Table I. The functional forms of the potentials are given in Table I of Ref. 3. The same functional form (the usual Thomas form) was used for both the real and imaginary  $\vec{L} \cdot \vec{S}$  potentials. The imaginary  $\vec{L} \cdot \vec{S}$  potential is about half as strong as the real  $\vec{L} \cdot \vec{S}$  term, and it tends to have a slightly larger radius parameter and a slightly smaller diffuseness. The other features of the potential, including the  $T_r$  tensor term, will be discussed in a subsequent paper.

The results of similar calculations for several nuclei (including those shown in Figs. 1 and 2) are summarized in Table II, which gives the parameters of the imaginary  $\vec{L} \cdot \vec{S}$  potential and

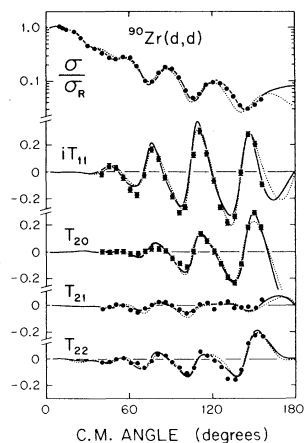


FIG. 2. Optical-model calculations for deuteron elastic scattering from <sup>90</sup>Zr at 15 MeV (Ref. 7). The curves have the same meaning as in Fig. 1.

TABLE I. Potential parameters for <sup>90</sup>Zr at 15 MeV, corresponding to the solid curves in Fig. 2.  $V$ ,  $R$ , and  $a$  are the depth, radius, and diffuseness parameters, respectively. The functional forms of the various potentials are given in Table I of Ref. 3. The real and imaginary  $\vec{L} \cdot \vec{S}$  potentials have the same functional form. The Coulomb radius is  $1.3A^{1/3}$  fm.

	$V$ (MeV)	$R$ (fm)	$a$ (fm)
Real central	91.6	1.20	0.78
Imaginary central	18.7	1.30	0.63
Real $\vec{L} \cdot \vec{S}$	4.2	0.62	0.48
Imaginary $\vec{L} \cdot \vec{S}$	2.4	0.69	0.28
Real $T_r$	0.5	1.7	1.1
Imaginary $T_r$	1.8	1.3	1.1

the value of  $\chi^2$  per measurement for fits with and without the imaginary  $\vec{L} \cdot \vec{S}$  term. Each data set consists of 105 to 146 measurements, including cross sections and all four analyzing powers. The improvement in  $\chi^2$  when an imaginary  $\vec{L} \cdot \vec{S}$  term is added ranges from 27% to 45%. The depth of the imaginary  $\vec{L} \cdot \vec{S}$  potential lies between 2.0 and 2.6 MeV in all but two anomalous cases.<sup>9</sup> This consistency is evidence that the improvements in the fits are not simply the result of adding adjustable parameters.

There is some theoretical justification for an imaginary  $\vec{L} \cdot \vec{S}$  potential. The existence of such

TABLE II. Imaginary  $\vec{L} \cdot \vec{S}$  parameters  $V$ ,  $R$ , and  $a$ , and goodness-of-fit parameters  $\chi_R^2$  and  $\chi_C^2$  (per measurement) for calculations with real and complex  $\vec{L} \cdot \vec{S}$  potentials, respectively.

Target	$E_d$ (MeV)	$V$ (MeV)	$R$ (fm)	$a$ (fm)	$\chi_R^2$	$\chi_C^2$	Ref.
<sup>46</sup> Ti	10	2.5	0.88	0.25 <sup>a</sup>	11.0	6.6	5, 6
<sup>52</sup> Cr	10	3.4	0.73	0.25 <sup>a</sup>	7.5	5.5	6
<sup>54</sup> Ni	10	3.7	0.81	0.25 <sup>a</sup>	5.6	3.9	6
<sup>68</sup> Zn	10	2.0	0.90	0.25 <sup>a</sup>	2.3	1.8	6
<sup>90</sup> Zr	10	2.2	0.62	0.25 <sup>a</sup>	3.9	2.6	6
<sup>52</sup> Cr	15	2.1	0.88	0.2 <sup>b</sup>	11.9	7.1	7
<sup>56</sup> Fe	15	2.2	0.83	0.2 <sup>b</sup>	7.0	4.9	7
<sup>60</sup> Ni	15	2.6	0.88	0.2 <sup>b</sup>	6.7	4.0	7
<sup>90</sup> Zr	15	2.4	0.69	0.28	6.6	3.6	7
<sup>122</sup> Sn	15	2.2	0.69	0.32	1.5	0.9	7

<sup>a</sup>The uncertainties in these diffusenesses are very large; so they were fixed at 0.25 to facilitate comparisons of the strengths.

<sup>b</sup>These diffusenesses reached the lower limit set by the search program, and were fixed there.

a potential implies that the absorption of flux out of the elastic channel is spin dependent. This is not surprising in view of the fact that the dominant reaction channels at these deuteron energies (stripping and inelastic scattering) are known to have fairly large analyzing powers.<sup>10,11</sup> Also, preliminary calculations by Rawitscher<sup>12</sup> indicate that a complex,  $L$ -dependent component of the  $\vec{L} \cdot \vec{S}$  potential is expected when deuteron breakup is considered in second-order Born approximation. Evidence for a complex  $\vec{L} \cdot \vec{S}$  potential has been obtained for deuteron-nucleus and proton-nucleus scattering at much higher energies ( $> 100$  MeV),<sup>13</sup> but it is not clear that these observations have any bearing on the present low-energy results.

In summary, the evidence for an imaginary  $\vec{L} \cdot \vec{S}$  potential is based on the following arguments: It solves a specific, identifiable problem—the relative angular shift between the cross section and  $iT_{11}$ —which has been seen in previous optical-model calculations (e.g., Ref. 1), and which has not been solved by any other means.<sup>14</sup> The same potential also improves the fits to the tensor analyzing powers, especially  $T_{22}$ . Furthermore, the strength of this new potential does not depend strongly on target mass or energy (excluding the anomalous  $N = 28$  nuclei). Therefore, we believe that the phenomenological evidence alone is sufficient to justify the addition of an imaginary  $\vec{L} \cdot \vec{S}$  potential to the deuteron-nucleus interaction.

Our thanks are extended to Professor Rawitscher for sending us his results before publication, and for other valuable comments. This work was supported in part by the U. S. Energy Research and Development Administration.

<sup>1</sup>J. M. Lohr and W. Haeberli, Nucl. Phys. A232, 381 (1974).

<sup>2</sup>F. D. Becchetti and G. W. Greenless, Phys. Rev. 182, 1190 (1969).

<sup>3</sup>P. W. Keaton, Jr., and D. D. Armstrong, Phys. Rev. C 8, 1692 (1973).

<sup>4</sup>The only exceptions are L. D. Knutson and W. Haeberli, Phys. Rev. C 12, 1469 (1975), who succeeded in fitting <sup>90</sup>Zr and <sup>208</sup>Pb data at energies below the Coulomb barrier, and H. R. Bürgi, W. Gruebler, P. A. Schmelzbach, V. König, and R. Risler, Nucl. Phys. A247, 322 (1975), whose calculations for <sup>40</sup>Ar ignored the off-diagonal ( $L \neq L'$ ) component of the  $T_r$  tensor potential, which is important for  $T_{21}$ .

<sup>5</sup>E. J. Stephenson, Ph.D. thesis, University of Wisconsin-Madison, 1975 (unpublished).

<sup>6</sup>R. P. Goddard and W. Haeberli, Bull. Am. Phys. Soc. 18, 1393 (1973).

<sup>7</sup>P. A. Hardekopf, D. D. Armstrong, L. L. Catlen, P. W. Keaton, Jr., and G. P. Lawrence, LASL Report No. LA-5051, 1972 (unpublished). The cross sections were renormalized by the following factors to improve the fits at forward angles: <sup>52</sup>Cr, 1.02; <sup>90</sup>Zr, 1.03; <sup>122</sup>Sn, 1.30.

<sup>8</sup>R. P. Goddard, "DOMINI: A Deuteron Optical Model Routine with Chi-Squared Minimization," 1977 (unpublished).

<sup>9</sup>Both of the anomalous cases, <sup>52</sup>Cr and <sup>54</sup>Fe, have a closed neutron shell ( $N = 28$ ), and both are characterized by an extreme forward shift in  $T_{22}$ , which is not well reproduced by the calculations.

<sup>10</sup>D. C. Kocher and W. Haeberli, Nucl. Phys. A196, 225 (1972).

<sup>11</sup>F. T. Baker, S. Davis, C. Glashauser, and A. B. Robbins, Nucl. Phys. A250, 79 (1975).

<sup>12</sup>G. Rawitscher, Bull. Am. Phys. Soc. 22, 597 (1977), and private communications. His predicted imaginary  $\vec{L} \cdot \vec{S}$  potentials are considerably smaller than ours.

<sup>13</sup>Deuteron-nucleus: L. J. Campbell, Nucl. Phys. 64, 273 (1965). Proton-nucleus: W. T. H. van Oers, Phys. Rev. C 3, 1550 (1971). Both of these papers find imaginary  $\vec{L} \cdot \vec{S}$  potentials with opposite sign from the one found here.

<sup>14</sup>O. Karban, A. K. Basak, J. A. R. Griffith, S. Roman, and G. Tungate, Nucl. Phys. A266, 413 (1976), briefly mentioned some exploratory calculations using an imaginary  $\vec{L} \cdot \vec{S}$  potential of unspecified strength. They noted an improvement in the fits to  $T_{20}$  and  $T_{22}$  for 12.4-MeV deuterons scattered from <sup>50</sup>Cr, <sup>66</sup>Zn, and <sup>67</sup>Zn.